Quantum tomography for time domain Balanced Homodyne Detection with high electronic noise

Martina Esposito[1], Daniele Fausti[1,2,*], Stefano Olivares[3], Fabio Benatti[1, 4], Roberto Floreanini[4], Fabio Novelli[1], Federico Cilento[2], Francesco Randi[1], and Fulvio Parmigiani[1, 2]

[1]Department of Physics, Università degli Studi d Trieste, 34127 Trieste, Italy
[2]Sincrotrone Trieste S.C.p.A., 34127 Basovizza, Italy
[3]Department of Physics, Università degli Studi di Milano, 20133 Milano, Italy
[4]Istituto Nazionale di Fisica Nucleare, Sezione di Trieste, 34151 Trieste, Italy
[*]Correspondence to [daniele.fausti@elettra.trieste.it]

Here we report on the design, construction and characterization of a time domain Balanced Homodyne Detection apparatus operating in the regime of high electronic noise. The experimental setup has been commissioned by studying coherent ultrashort (~ 80 fs) light pulses using Pattern-function Quantum Tomography. Furthermore, we proved that the electronic noise can be treated as a detector inefficiency showing the effectiveness of this approach by measuring light coherent states with different energies.

In Quantum Mechanics *the measurement of the state* of a physical system implies to estimate the expectation value of any observable of the system. For a generic operator the expectation value is obtained starting from the measurement of an ensemble of observables defined "quorum"[1]. In particular, for the electromagnetic field the quorum is a continuum set of the field quadratures[2,3].

Balanced Homodyne Detection (BHD) is an experimental method for measuring a discrete set of the field quadratures for a single mode cw field[4–7]. Such measurements can be analyzed by the Pattern-function Quantum Tomography (PFQT) technique in order to characterize the quantum state of the optical mode[8].

Instead, for pulsed radiation fields a BHD operating in the time domain must be used[9–15]. In this case the optical pulses are equally prepared quantum states and the set of measurements fed to PFQT comprises single pulse quadrature measurements. Although this is a standard method in quantum information, its effectiveness under high noise condition has to be proven.

Here we report the characterization of a time domain BHD apparatus operating in a regime of high electronic noise (EN). We treat the low shot-to-electronic-noise ratio (≈ 0.8 dB) as a detector inefficiency[16]. In order to prove the applicability of this treatment to high EN homodyne detection, the PFQT technique has been exploited. The expectation value of the number operator of pulsed coherent states with different energies has been found consistent with the measured mean number of photons per pulse. Furthermore, the analyzed states are confirmed to be Gaussian and minimum uncertainty states.

Results

In BHD the *signal*, i. e. the field under investigation, is mixed with a strong coherent reference field, the local oscillator (LO), by a 50/50 beam splitter. The outputs are collected by two photodiodes and the difference photocurrent (homodyne photocurrent) is measured. It can be proven that, when the LO is significantly more intense than the *signal*, the homodyne photocurrent is proportional to the *signal* field quadrature[17]. Given $\hat{a}$ and $\hat{a}^\dagger$ the field operators associated with the optical mode of the *signal*, the quadrature operator is defined as:

$$\hat{x}_\Phi = \frac{(\hat{a}e^{-i\Phi} + \hat{a}^\dagger e^{i\Phi})}{\sqrt{2}}, \qquad (1)$$

where Φ is the relative phase between the *signal* and the LO. The continuum set of quadratures with $\Phi \in [0, 2\pi]$ constitutes a quorum characterizing the *signal* mode. Noteworthy the concept of light mode, usually associated with a monochromatic field, needs to be generalized for pulsed light. A thorough theoretical treatment for BHD in pulsed regime is presented herewith in the Methods section.

The opto-mechanical scheme of our experimental apparatus is shown in Fig. 1. The laser source is a mode-locked Ti:Sapphire oscillator with 80 MHz repetition rate. A beam splitter divides the incoming beam in two parts which then interfere in a second beam splitter (NPBS in Fig. 1). The outputs are detected and subtracted by a differential photodetector (*Thorlabs PDB430A*). The latter is made up of two Si/PIN photodiodes with nominal quantum efficiency of 0.77. We verified that the response of the photodiodes is linear up to 0.6 mW LO power, while a non-linear response sets in at higher powers. The detector subtraction efficiency is quantified by the common mode rejection

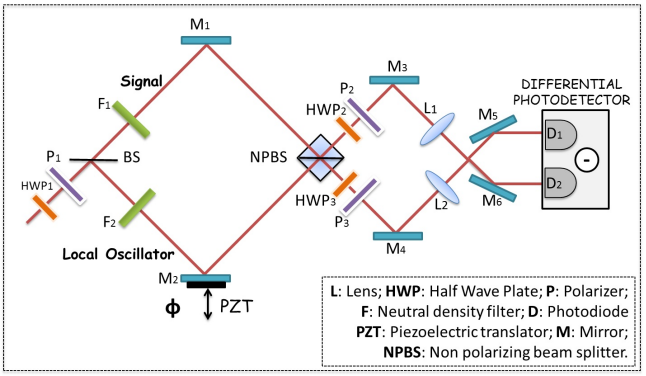

Figure 1: Scheme of the opto-mechanical setup.

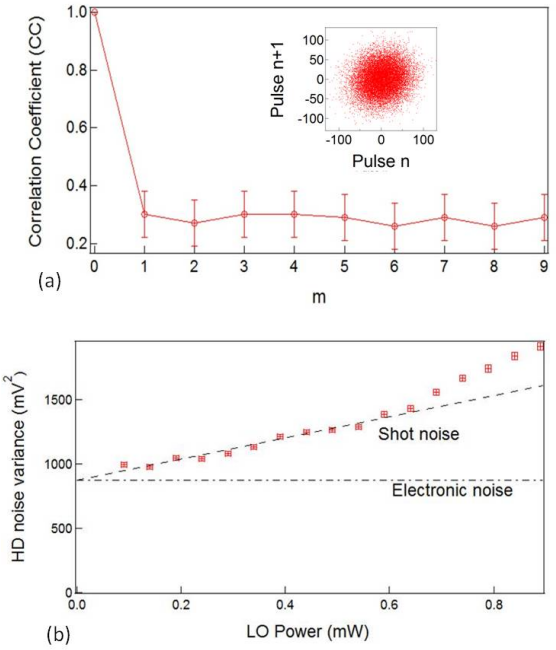

Figure 2: Detector characterization measurements. (a) Correlation coefficient between pulse n and $n+m$ (LO power: 0.6 mW). Inset: parametric plot of 2×10^4 subsequent pulses where the pulse n+1 is plotted against the pulse n. (b) HD noise variance versus LO power; shot noise contribution (dashed curve); electronic noise background (dashed-dotted curve).

ratio (CMRR), defined as the ratio between the detector output power when both photodiodes are illuminated and the power when one of the two is screened. The measured CMRR for our apparatus is larger than 36 dB.

The homodyne photocurrent is recorded by a digital oscilloscope (*Tektronix TDS3000B*) with a bandwidth of 500 MHz and a sampling rate of 5 GSamples/s. The digitized output is numerically integrated over time intervals corresponding to the duration of the pulse. Each integral is associated with a single quadrature measurement. We checked the independence of each quadrature measurement by performing a correlation test between two subsequent pulses. The Correlation Coefficients (CCs) [14] between pulse n and $n+m$ ($m = 0, 1...9$) are shown in Fig. 2 (a). In the inset a parametric plot of 2×10^4 subsequent pulses is shown, where the pulse $n+1$ is plotted against the pulse n. The weak correlation in this plot demonstrates that there is no significant impact on the measured integral of the pulse $n+1$ from that of the pulse n. Each CC in Fig. 2 (a) is calculated using the data obtained from 200 difference pulses. The CC between pulse n and pulse $n+1$ is 0.30 ± 0.08; this value is slightly higher with respect to other reported BHDs, i. e. smaller than 0.1 [12–15]. We can conclude that there is a small correlation between adjacent pulses, since the CC has approximately the same value for $m = 2, ...9$. This could be attributed to noise at a frequency lower than the repetition rate of the pulses.

In *shot noise regime* the homodyne detector (HD) noise variance is expected to change linearly in the LO power with a constant offset representing the electronic noise [18]. We calculated the HD noise variance of 8×10^3 pulses for different values of the LO power. The result is shown in Fig. 2 (b): the HD noise variance contains an electronic background and a linear contribution up to 0.6 mW LO power; for higher powers the non-linear effects due to the photodiodes start. We work at 0.6 mW LO oscillator power in order to have the maximum shot-to-electronic noise ratio ($S = 1.2$) achievable in the linear regime. The measurements reported in Fig. 2 are obtained with the *signal* beam blocked, i.e. with the *signal* in the vacuum state.

When the *signal* beam is not blocked, it is attenuated with respect to the LO by means of a neutral density filter (F_1 in Fig. 1). The phase difference Φ between the two arms of the interferometer can be modulated in the $[0, 2\pi]$ range using a piezoelectric translator in the LO arm (PZT in Fig. 1). The homodyne photocurrent is acquired by the digital oscilloscope and each difference pulse is integrated. The obtained value N_i, corresponding to a certain piezo position p_i, is proportional to a quadrature measurement x_Φ:

$$N_i = \gamma\, x_\Phi. \tag{2}$$

The proportionality factor γ is obtained using the vacuum state as a reference. This is allowed since the quadrature variance for the vacuum state is $\sigma^2[\hat{x}_\Phi]_{|0\rangle} = 1/2$ for any phase value. Defining γ as:

$$\gamma = \sqrt{2\,\langle N_{i0}^2 \rangle}, \tag{3}$$

the vacuum homodyne measurement has been used to extract the N_{i0} values. $\langle N_{i0}^2 \rangle$ is the variance of 8×10^4 experimental data of the vacuum. The homodyne data have been calibrated dividing N_i by γ. Note that γ will give a misleading estimation of the actual mean photon number. Therefore, a correction taking into account the EN effect is necessary, as discussed in the following. The calibrated measurements for three optical coherent states with different energies are reported in Fig. 3. The optical density OD of the filter F_1 used for each measurement is given in the caption. The homodyne traces are composed of $M = 8 \times 10^4$ experimental data:

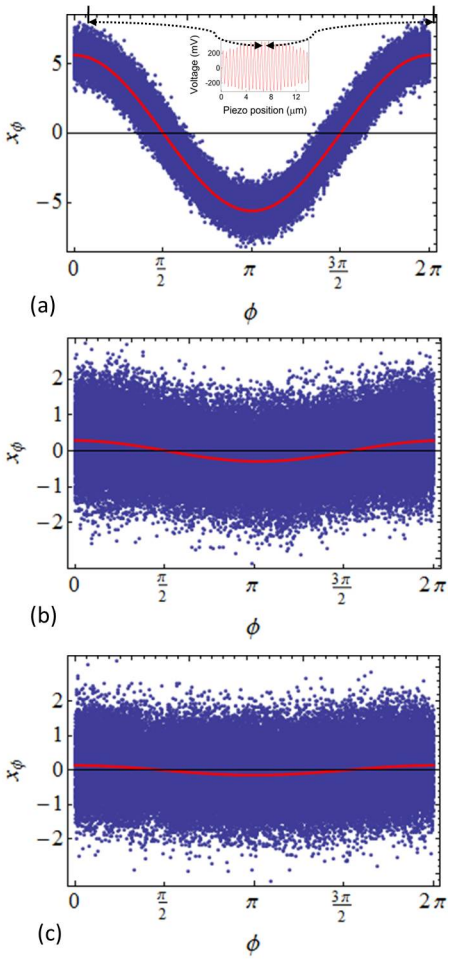

Figure 3: Homodyne traces of three optical coherent states. Each trace is acquired using a different optical density OD of the filter F_1. (a) $OD = 4.5$; (b) $OD = 7$; (c) $OD = 8$. In the inset of (a) we show the interference figure obtained by measuring the mean value of 4 integrated pulses versus the piezo position. The homodyne traces are measured in the piezo range corresponding to the central optical cycle of the interference figure.

$\{(x_1;\Phi_1),(x_2;\Phi_2),...,(x_k;\Phi_k),...,(x_M;\Phi_M)\}$.
However, the effect of the EN, which adds a random quantity to each field quadrature measurement, must be accounted for. Appel at al. demonstrate [16] that this noise can be treated as an optical loss channel with equivalent transmission efficiency,

$$\eta_{eq} = 1 - \frac{1}{S}, \tag{4}$$

where S is the ratio between shot and electronic noise at the chosen LO power. In particular, the vacuum state measurement is distorted by the EN and consequently the rescaling factor γ must be changed. Following the Appel's treatment [16] and considering equation (3), the following expression is obtained,

$$\gamma' = \sqrt{\eta_{eq}}\,\gamma, \tag{5}$$

where γ' is the conversion factor in case of absence of electronic noise. Thus, in order to take into account the EN, the homodyne data have been normalized to γ'.

These data have been used to characterize the quantum state of the *signal* field via PFQT [8].

Discussions

The PFQT technique can be summarized as follows. For a generic observable $\hat{O}$ of the optical mode it is possible to find a *pattern function* $R_{\hat{O}}(x;\Phi)$ for which the statistical average over the experimental data,

$$S_M = \frac{1}{M}\sum_{k=1}^{M} R_{\hat{O}}(x_k;\Phi_k), \tag{6}$$

gives an estimation of the expectation value $\langle\hat{O}\rangle$ with an error

$$\epsilon_M = \sqrt{\frac{\sum_{k=1}^{M}[R_{\hat{O}}(x_k;\Phi_k) - S_M]^2}{M(M-1)}}. \tag{7}$$

This technique is used to estimate the expectation value of the number operator $(\hat{a}^\dagger\hat{a})$, which can be evaluated in an independent way.
The pattern function of the number operator is:

$$R_{\hat{a}^\dagger\hat{a}}(x_\Phi;\Phi) = (x_\Phi)^2 - \frac{1}{2\eta}, \tag{8}$$

where the factor η is the quantum efficiency of the homodyne detection apparatus. In order to take into account the EN loss effect, we put $\eta = \eta_{eq}$ given in equation (4). Finally we estimate the mean photon number as:

$$\langle\hat{n}\rangle_{PFQT} = \frac{1}{M}\sum_{k=1}^{M} R_{\hat{a}^\dagger\hat{a}}(x_k;\Phi_k)\,\frac{1}{\eta_{eq}}. \tag{9}$$

The error on this estimation is calculated using equation (7). The results for the three different homodyne traces are reported in Table 1. The expectation values

OD	$\langle\hat{n}\rangle_{PFQT}$
4.5	596 ± 2
7	1.6 ± 0.1
8	0.6 ± 0.1

Table 1: Expectation values of the number operator of three optical coherent states for three different optical densities ODs. The values are obtained via PFQT from the homodyne measurements reported in Fig. 3 taking into account the equivalent quantum efficiency η_{eq} as in equation (4).

calculated using the PFQT are consistent, in the order of magnitude, with the mean number of photons per pulse obtained from the nominal OD of the filter. In this way we verify that the treatment of low EN [16] is valid also for high EN detection systems.
Now we focus on the optical state with the lowest energy [Fig. 3 (c)]. The analysis for the other states is analogous.

First we verify the Gaussianity of the experimental data through the evaluation of the *kurtosis excess* κ, which is zero for Gaussian distributions[19]. Considering 10^3 experimental data in the first phase range of the homodyne trace in Fig. 3 (c) and we obtain a *kurtosis excess* $\kappa = -0.008$. Since all the phase ranges lead to a $\kappa \approx 0$, this proves the Gaussianity of the homodyne probability distribution function.
Then we use the PFQT to evaluate the expectation values of the the two quadratures associated with the position and momentum operators ($\hat{x}_{(\Phi=0)} = \hat{q}$; $\hat{x}_{(\Phi=\pi/2)} = \hat{p}$) and of their variances ($\sigma^2[\hat{q}]$; $\sigma^2[\hat{p}]$). The results, shown in Table 2, demonstrate that the analyzed state is a minimum uncertainty state.

$\langle\hat{q}\rangle$	$\sigma^2[\hat{q}]$
0.36 ± 0.01	0.53 ± 0.05
$\langle\hat{p}\rangle$	$\sigma^2[\hat{p}]$
0.00 ± 0.01	0.53 ± 0.05

Table 2: Expectation values of the position and momentum operators and their variances. The values are obtained via PFQT from the homodyne measurements reported in Fig. 3 (c).

Finally we evaluate the covariance matrix C, that fully characterizes Gaussian states and directly depends on the field quadratures[20]. The elements of the covariance matrix are defined as:

$$C_{kj} = \frac{1}{2}\langle\{\hat{R}_k, \hat{R}_j\}\rangle - \langle\hat{R}_j\rangle\langle\hat{R}_k\rangle\,, \tag{10}$$

where $\hat{R} = (\hat{q}, \hat{p})$ is the *first-moments vector* of the optical state and $\{\hat{A}, \hat{B}\} = \hat{A}\hat{B} + \hat{B}\hat{A}$ is the anti-commutator between two operators[20]. From the PFQT we obtain the following estimations:

$$C = \begin{pmatrix} 0.53 \pm 0.5 & -0.02 \pm 0.03 \\ -0.02 \pm 0.03 & 0.53 \pm 0.05 \end{pmatrix}. \tag{11}$$

This is consistent with what is expected for a coherent state. The other two homodyne measurements, reported in Fig. 3 (a) and (b), lead to similar results.

In conclusion, we reported the characterization of a time domain BHD apparatus operating in the high electronic noise regime. The apparatus has been characterized via the PFQT of optical coherent states with different mean number of photons per pulse. We treated the electronic noise trough the approach used by Appel at al.[16] and we showed that such a treatment is valid for high EN homodyne detectors. This result is of relevance in the perspective of using BHD and PFQT in experiments performed in high noise environments such as time domain pump-probe spectroscopy. In particular, ultrashort light pulses could be used to prepare coherent states into matter and BHD to have a full characterization of the light pulses which have interacted with transient matter states.

Methods

BHD theoretical treatment in the pulsed regime. BHD in a pulsed regime requires a formal generalization of its theoretical description with respect to the one-mode regime; indeed, the *LO* and the *signal* at the beam splitter are not monochromatic. Classically, the electric field of a pulsed laser beam is in a mode-locked superposition of amplitudes:

$$E(t) = \sum_{l=-M}^{M} |\alpha_l|\, e^{i\,\Phi_l(t)}\ ,\ \Phi_l(t) = \omega_l\, t + \varphi_l\ , \tag{12}$$

where the phases $\Phi_l(t)$ are mode-locked by the condition $\varphi_l = l\,\varphi_0$. Each frequency ω_l contributes to the field with the amplitude $\alpha_l = |\alpha_l|\, e^{i\Phi_l}$ and the number of contributing frequencies depends on the shape of the pulse. Quantized pulsed laser light is described by associating to each monochromatic component a coherent state $|\alpha_l\rangle$, that is an eigenstate of the annihilation operator $\hat{a}_l$ of photons in the mode of frequency ω_l, $\hat{a}_l\,|\alpha_l\rangle = \alpha_l\,|\alpha_l\rangle$, and to the entire pulse the tensor product

$$|\bar{\alpha}\rangle = \bigotimes_{l=-M}^{M} |\alpha_l\rangle\,, \tag{13}$$

where $\bar{\alpha}$ is the vector whose components are the amplitudes α_l. By means of the creation and annihilation operators $\hat{a}$ and $\hat{a}_l^\dagger$ each monochromatic coherent state reads

$$|\alpha_l\rangle = D(\alpha_l)\,|0\rangle\ ,\ D(\alpha_l) = e^{\alpha_l \hat{a}_l^\dagger - \alpha_l^* \hat{a}_l}\ , \tag{14}$$

where $|0\rangle$ is the vacuum state and $D(\alpha)$ is the so-called displacement operator.
Since the creation and annihilation operators pertaining to different modes commute, the pulsed coherent state (13) can conveniently be recast as:

$$|\bar{\alpha}\rangle = D(\bar{\alpha})\,|0\rangle\ ,\ D(\bar{\alpha}) = e^{\hat{A}^\dagger(\bar{\alpha}) - \hat{A}(\bar{\alpha})}\ , \tag{15}$$

in terms of a multi-mode displacement operator $D(\bar{\alpha})$ where

$$\hat{A}^\dagger(\bar{\alpha}) = \sum_l \alpha_l\, \hat{a}_l^\dagger\ ,\quad \hat{A}(\bar{\alpha}) = \sum_l \alpha_l^*\, \hat{a}_l\ . \tag{16}$$

The reason for labeling the pulsed coherent state by $|\bar{\alpha}\rangle$ can now be easily understood. The state of one photon of frequency ω_l is given by $\hat{a}_l^\dagger\,|0\rangle = |1_l\rangle$, while a generic non-monochromatic superposition of frequencies ω_l with amplitudes α_l corresponds to the state $|1_{\bar{\alpha}}\rangle = \sum_l \alpha_l\,|1_l\rangle$ that results from

$$\hat{A}^\dagger(\bar{\alpha})\,|0\rangle = \sum_l \alpha_l\, \hat{a}_l^\dagger\,|0\rangle = \sum_l \alpha_l\ |1_l\rangle = |1_{\bar{\alpha}}\rangle\,. \tag{17}$$

Therefore, $\hat{A}^\dagger(\bar{\alpha})$ is the creator operator of a single-photon in the (not normalized) superposition state $|1_{\bar{\alpha}}\rangle$, while $\hat{A}(\bar{\alpha})$ destroys a photon in the same state; thus, the quantum state of the pulsed laser is a coherent state associated not with a single amplitude α_l, but with the vector $\bar{\alpha}$ of all the amplitudes contributing

to the pulse: in other words, we have a Poissonian distribution not with respect to the number of photons in a monochromatic wave, but to the number of photons in the superposition $|1_{\bar{\alpha}}\rangle$.
The normalized operators

$$\hat{A} = \frac{\hat{A}(\bar{\alpha})}{|\bar{\alpha}|} \ , \quad \hat{A}^\dagger = \frac{\hat{A}(\bar{\alpha})}{|\bar{\alpha}|} \ , \tag{18}$$

where $|\bar{\alpha}|^2 = \langle 1_{\bar{\alpha}}|1_{\bar{\alpha}}\rangle$, satisfy the canonical commutation relations

$$\left[\hat{A}, \hat{A}^\dagger\right] = \frac{1}{|\bar{\alpha}|^2} \sum_{ij} \alpha_i^* \alpha_j \, [\hat{a}_i, \hat{a}_j^\dagger] = 1 \ . \tag{19}$$

By means of them we can now extend the state-tomography techniques to the case in which the *signal* and the *LO* are pulsed. In the monochromatic case, when the *signal* mode a interferes with the *LO* mode b on the beam splitter, the photo-current operator is $\hat{I} = \hat{a}^\dagger \hat{b} + \hat{b}^\dagger \hat{a}$ [17].
If more frequencies ω_l are present both in the *LO* and in the *signal*, each one of the corresponding mode operators will be subjected to the beam splitting transformation and the detectors will ideally register photons of all involved frequencies. Then, the photo-current operator becomes $\hat{I} = \sum_l \hat{a}_l^\dagger \hat{b}_l + \hat{b}_l^\dagger \hat{a}_l$.

If the *LO* incoming field is in a pulsed coherent state $|\bar{z}\rangle = e^{\hat{B}^\dagger(\bar{z}) - \hat{B}(\bar{z})} |0\rangle$, with generalized creation and annihilation operators $\hat{B}^\dagger(\bar{z}) = \sum_l z_l \hat{b}_l^\dagger$ and $\hat{B}(\bar{z}) = \sum_l z_l^* \hat{b}_l$, the phase difference Φ between the *LO* and the *signal* is changed by the action of the piezoelectric translator placed in the *LO* arm on all the *LO* modes:

$$\hat{b}_l \to \hat{b}_l \, e^{i\Phi} \ , \quad \hat{b}_l^\dagger \to \hat{b}_l^\dagger \, e^{-i\Phi} \ . \tag{20}$$

The photo-current operator which is measured by the pulsed homodyne setup is thus given by

$$\hat{I}_\Phi = \sum_l \left(\hat{a}_l^\dagger \, \hat{b}_l \, e^{i\Phi} \, + \, \hat{a}_l \, \hat{b}_l^\dagger \, e^{-i\Phi} \right) \ . \tag{21}$$

Let $\hat{\rho}_s$ denote the quantum state (density matrix) of the *signal* field and by $|\bar{z}\rangle \langle \bar{z}|$ the projector onto the (coherent) state of the incoming pulse. Then, using that $\hat{b}_l \, |\bar{z}\rangle = z_l \, |\bar{z}\rangle$ and the expressions in (16), the expectation value $I_\Phi = \mathrm{Tr}\left(\rho_s \otimes |\bar{z}\rangle \langle \bar{z}| \, \hat{I}_\Phi \right)$ of the photo-current is calculated as follows:

$$\begin{aligned} I_\Phi &= \sum_l \left(\mathrm{Tr}\left[\hat{\rho}_s \, \hat{a}_l^\dagger \right] \cdot \langle \bar{z}|\hat{b}_l|\bar{z}\rangle \, e^{i\Phi} + h.c. \right) \\ &= \sum_l \left(\mathrm{Tr}\left[\hat{\rho}_s \, (\hat{a}_l^\dagger \, z_l \, e^{i\Phi} + \hat{a}_l \, z_l^* \, e^{-i\Phi}) \right] \right) \\ &= \mathrm{Tr}\left[\hat{\rho}_s \, \left(\hat{A}^\dagger(\bar{z}) \, e^{i\Phi} + \hat{A}(\bar{z}) \, e^{-i\Phi} \right) \right] \ . \end{aligned} \tag{22}$$

Using (18) and comparing these results in the standard treatment of BHD for the single-mode case, one realizes that the pulsed BHD measures a quantity I_Φ proportional to a quadrature which generalizes that in (1):

$$I_\Phi = \sqrt{2} \, |\bar{z}| \, \mathrm{Tr}\left[\hat{\rho}_s \, \hat{X}_\Phi \right] \ , \ \hat{X}_\Phi = \frac{\hat{A}^\dagger \, e^{i\Phi} + \hat{A} \, e^{-i\Phi}}{\sqrt{2}} \ . \tag{23}$$

For this reason, in the main text of the letter we have limited the discussion to the simpler case of a single mode BHD, with the proviso that whenever a quadrature is used, it actually refers to its expression in the pulsed regime. In particular, the measured data can be used to reconstruct the expectation values of all *signal* observables that can be expressed as functions of the operators $\hat{A}$ and $\hat{A}^\dagger$. For instance, the mean value of the photo-current operator second moment with respect to the *LO* pulsed coherent state $|\bar{z}\rangle \langle \bar{z}|$ is

$$\langle \bar{z}| \, \hat{I}_\Phi^2 \, |\bar{z}\rangle = 2 \, |\bar{z}|^2 \, \hat{X}_\Phi^2 \, + \, \sum_l \hat{a}_l^\dagger \hat{a}_l \tag{24}$$

and differs from the pulsed quadrature second moment $\hat{X}_\Phi^2$ by the number of photons in the pulsed *signal* which is to be taken much smaller than the intensity $|\bar{z}|^2$ of the pulsed *LO*. A similar suppression by $|\bar{z}|^{-2}$ occurs for the correction terms appearing in higher moments so that the distribution of the outcomes of the homodyne photocurrent is equal to that of the corresponding field quadratures.

Notice that, in the case of only one frequency mode, the above setting reduces to the standard homodyne tomographic techniques. Therefore, in conclusion, we have generalized the treatment of a monochromatic BHD to the case of pulsed input light. It explicitly takes into account the fact that the state of a pulsed laser is the tensor product of the coherent states of each contributing frequency.

Acknowledgement

Useful discussions with Simone Cialdi and Marco Barbieri are acknowledged. This work has been supported by MIUR (FIRB "LiCHIS"-RBFR10YQ3H), University of Trieste ("FRA 2009" and "FRA 2011") and European Union, Seventh Framework Programme, under the project GO FAST, grant agreement no. 280555.

References

1. Fano, U. Description of states in quantum mechanics by density matrix and operator techniques. *Reviews of Modern* **29**, 74 (1957).

2. Lvovsky & Raymer Continuous-variable optical quantum-state tomography. *Reviews of Modern Physics* **81**, 299 (2009).

3. Leonhardt, U. *Measuring the Quantum State of Light* (Cambridge Studies in Modern Optics, 1997).

4. Vogel, K. & Risken, H. Determination of quasiprobability distributions in terms of probability distributions for the rotated quadrature phase. *Phys.Rev. A* **40**, 2847 (1989).

5. Smithey, D. T., Beck, M., Raymer, M. G. & Faridani, A. Measurement of the Wigner distribution and the density matrix of a light mode using optical homodyne tomography: Application to squeezed

states and the vacuum. *Phys. Rev. A* **70**, 1244 (1993).

6. Welsch, Vogel & Opatrny Homodyne Detection and Quantum State Reconstruction. *Progress in Optics* **39**, 63 (1999).

7. Zavatta, Viciani & Bellini Non-classical field characterization by high-frequency,time-domain quantum homodyne tomography. *Laser Phys. Lett.* **3**, 3 (2006).

8. D'Ariano, Paris & Sacchi Quantum tomography. *Advances in Imaging and Electron Physics* **128**, 205 (2003).

9. Hansen *et al.* An ultra-sensitive pulsed balanced homodyne detector: Application to time-domain quantum measurements. *Optics letter* **26**, 1714 (2001).

10. Zavatta, Bellini, Ramazza, Marin & Arecchi Time domain analysis of quantum states of light: noise characterization and homodyne tomography. *J. Opt. Soc. Am. B* **19**, 1189 (2002).

11. Kumar *et al.* Versatile Wideband Balanced Detector for Quantum Optical Homodyne Tomography. *Optics Communications* **285** (2012).

12. Haderka, Michálek, Urbášek & Ježek Fast time domain balanced homodyne detection of light. *Applied Optics* **48**, 2884 (2009).

13. Cooper, Soller & Smith High-stability time domain balanced homodyne detector for ultrafast optical pulse applications. *Conference Paper: Quantum Electronics and Laser Science Conference* (QELS) San Jose, California (May, 2012).

14. Chi *et al.* A balanced homodyne detector for high rate Gaussian-modulated coherent-state quantum key distribution. *New Journal of Physics* **13** (2011).

15. Okubo, Hirano, Zhang & Hirano Pulse-resolved measurement of quadrature phase amplitudes of squeezed pulse trains at a repetition rate of 76 MHz. *Opt. Lett.* **33**, 1458 (2008).

16. Appel, Hoffman, Figueroa & Lvovsky Electronic noise in optical homodyne tomography. *Physical Review A* **75**, 035802 (2007).

17. Ferraro, A., Olivares, S. & Paris, M., *Gaussian states in quantum information* (Bibiopolis, Napoli,2005).

18. Bachor, H. A. & Ralph, T. C., *A Guide to experiments in Quantum Optics* (WileY-VCH, 2004).

19. Buono *et al.* Quantum characterization of bipartite Gaussian states. *J. Opt. Soc. Am. B* **27**, Section 5 (2010).

20. Olivares, S. Quantum optics in the phase space. *The European Physics Journal Special Topics* **203**, 3 (2012).